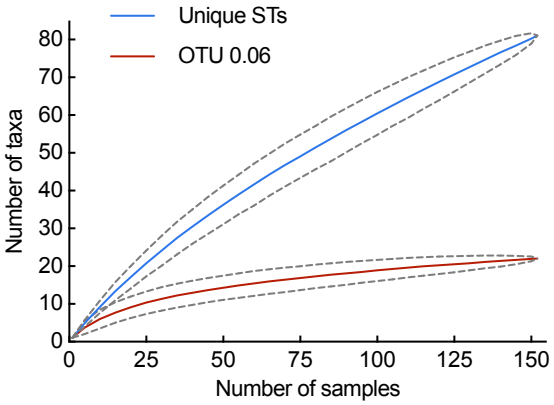

Figure 1. Rarefaction curves showing a near saturation of bacterial sampling.

Each curve represents the mean of 1000 replicates. Data of 95% confidence intervals are displayed with discontinuous lines.

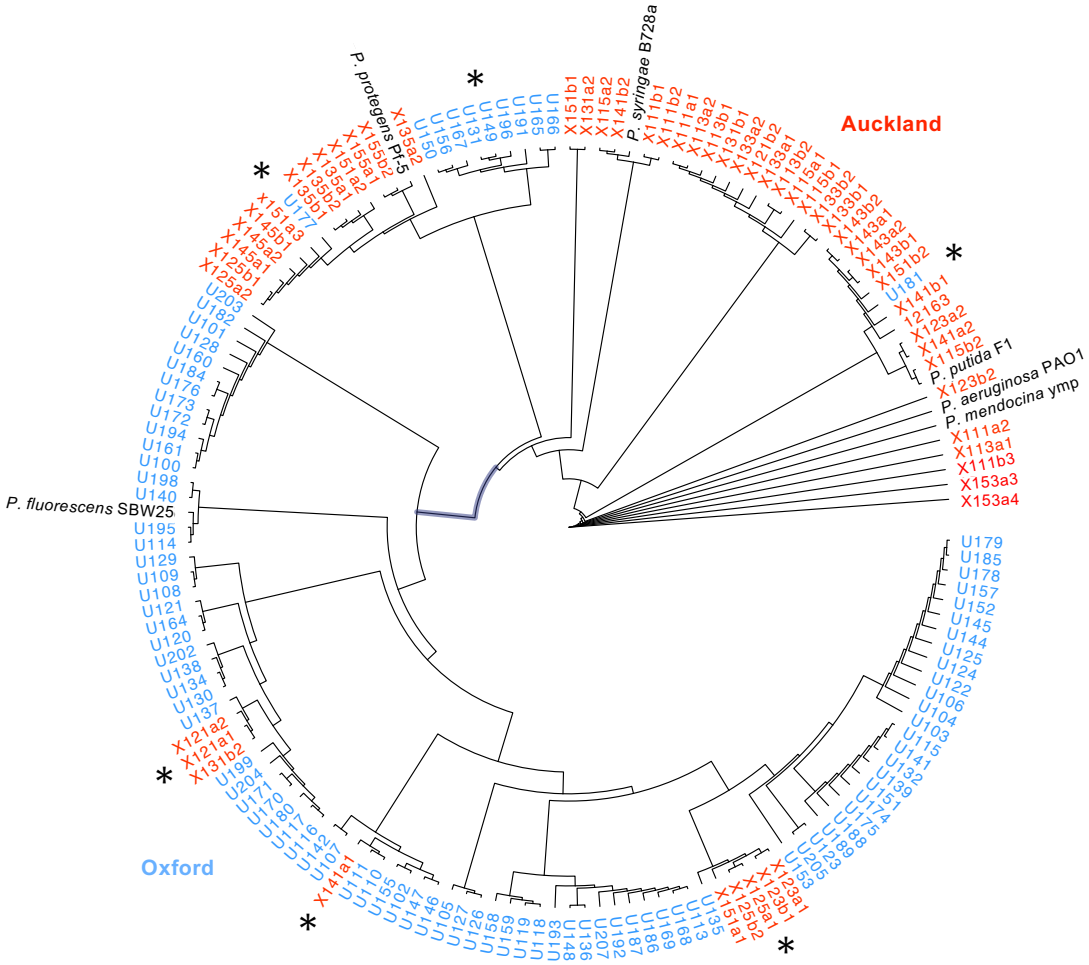

Figure 2. Phylogenetic relationships of sugar beet-associated *Pseudomonas*.

Isolates from Oxford and Auckland are differentiated by blue and red colors, respectively. Six reference *Pseudomonas* species were included in the analysis. Asterisks indicate the few Oxford isolates in the Auckland cluster, and vice versa.

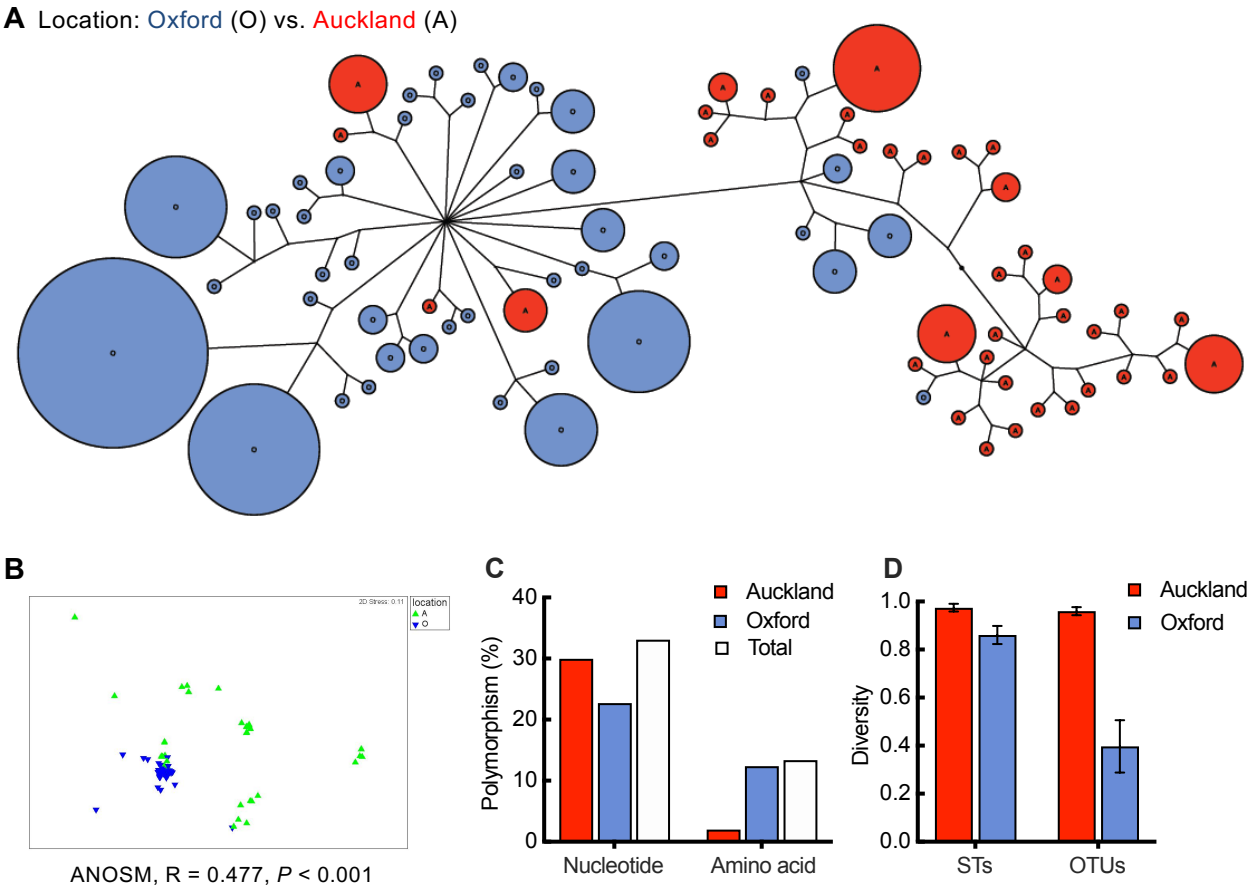

Figure 3. Comparative analysis of *Pseudomonas* isolated from Oxford and Auckland

A. Clonal frame output displayed as an unrooted network, indicating the origination of isolation. Distance was calculated using the NJ method with Kimura 2 correction. Sizes of the circles are proportional to the number of isolates.
B. Multi-dimensional scaling plot showing separation of *Pseudomonas* from Oxford (blue) and Auckland (green).
C. Nucleotide and amino acid polymorphism of the concatenated sequences by location.
D. Simpson's index of diversity (1-D) calculated on the basis of unique STs and OTUs clustered at the level of 0.06. Error bars are 95% CIs.

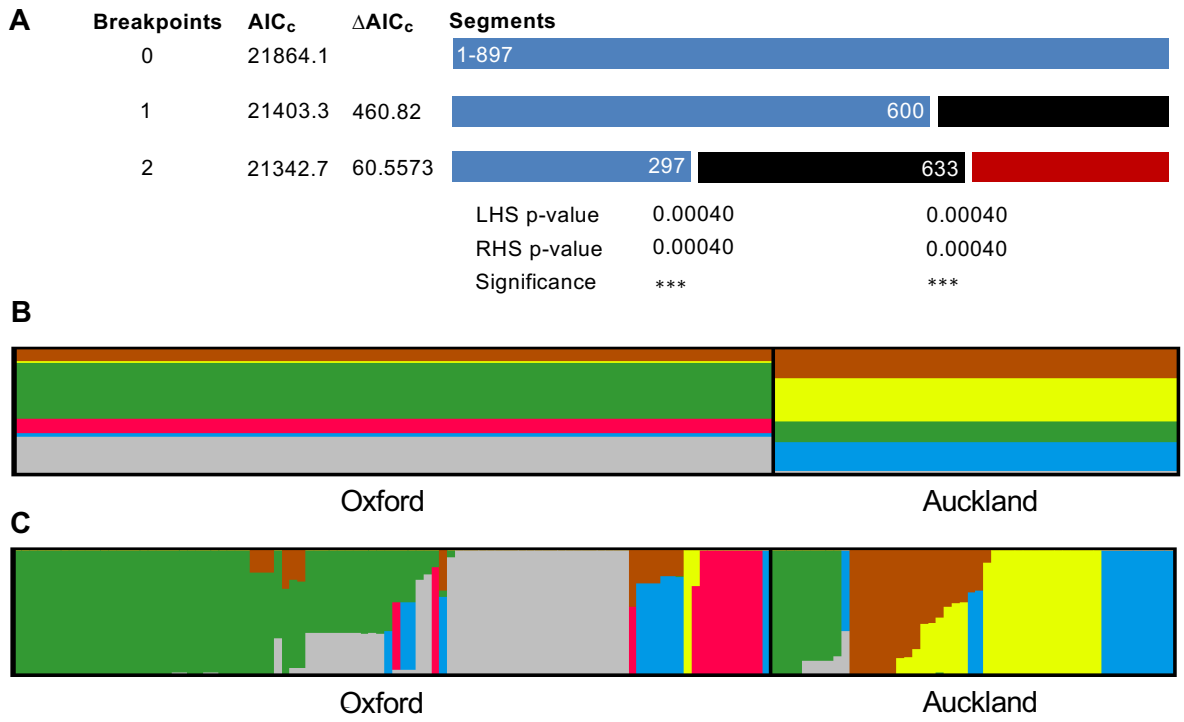

Figure 4. Evidence of recombination and structure of the Oxford and Auckland subpopulations.

A. Recombination breakpoints were detected using the method of GARD. Results of the Kishino-Hasegawa (KH) test are shown below the two detected breakpoints.
B. Distribution of the six "ancestral" genotypes revealed by STRUCTURE analysis.
C. Individual isolates sharing ancestry for the Oxford and Auckland subpopulations.

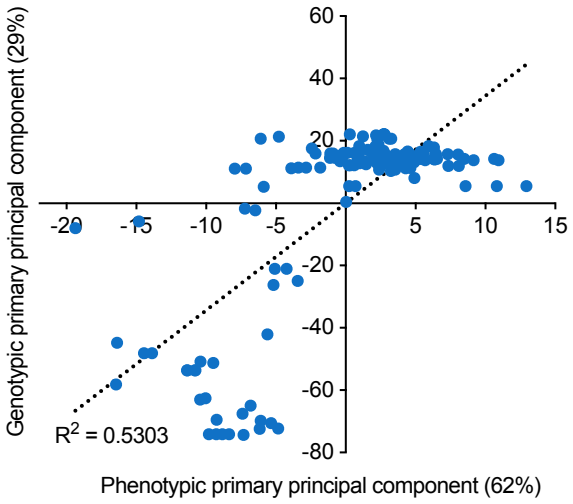

Figure 5. Principal component analysis showing correlations between genotypes and phenotypes.

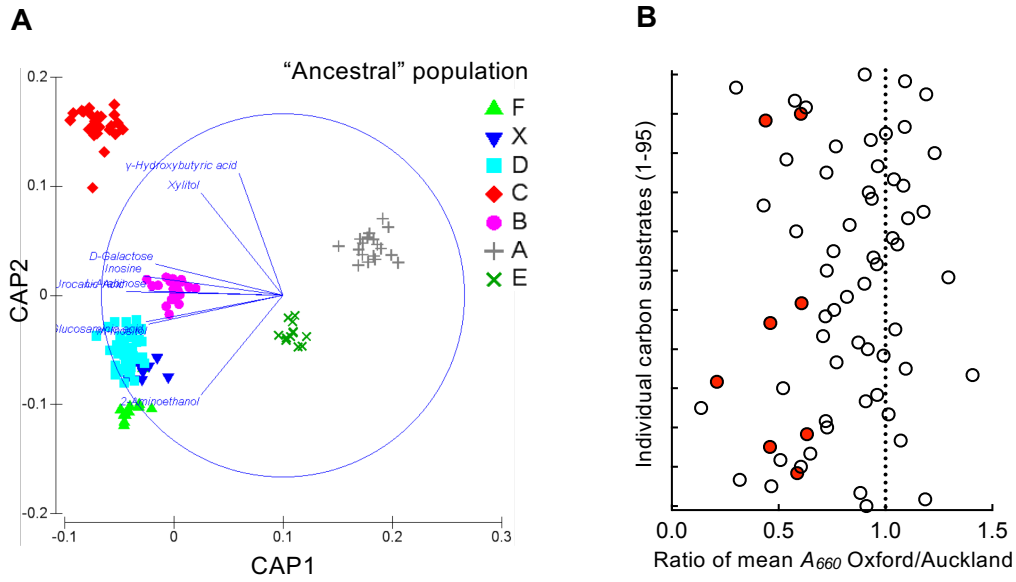

Figure 6. Genotypic relatedness of carbon source utilization (A) and the role of individual substrate in separating pseudomonads from Oxford and Auckland (B).

A. Canonical analysis of principal coordinates (CAP) based on a Euclidean distance similarity matrix generated from the Biolog and MLSA data. The six "ancestral" populations revealed by STRUCTURE analysis are indicated as A to E, while X denotes the other ancestral types. Only carbon substrates with *r* value larger than 0.8 are shown. A to E denotes the six an
B. Ratio of the mean value of bacterial growth (A_{660}) on each carbon source was calculated for isolates from Oxford and Auckland. The carbon substrates are listed in *y*-axis in order of their location in the Biolog GN2 MicroPlate from A2 to H12 labelled from number 1 to 95. Red circles denote the eight carbon substrates of strong correlation with genotypes (Fig. 6B).

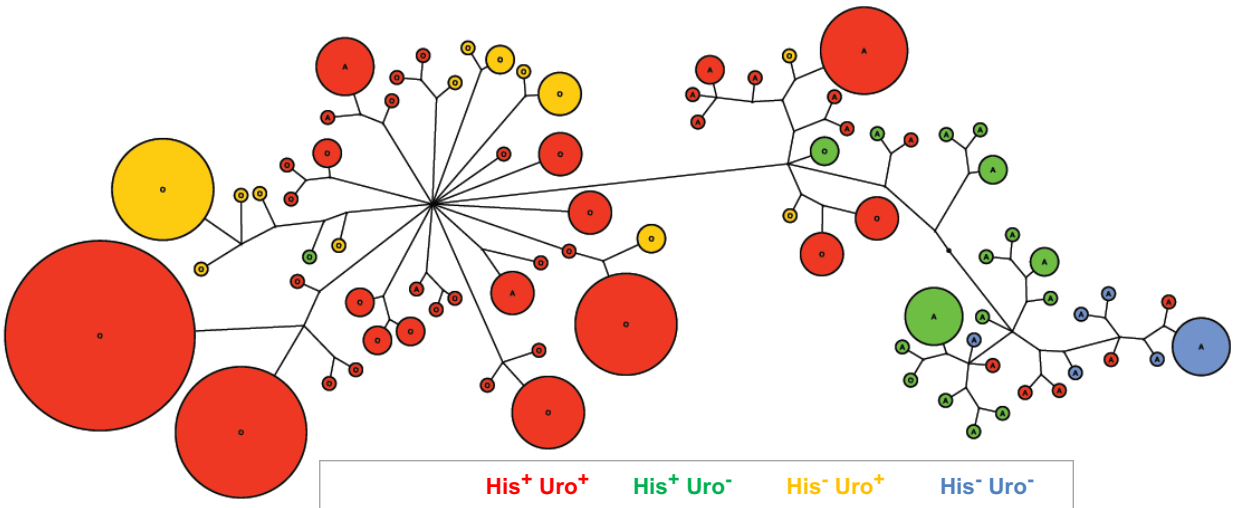

	$His^+ Uro^+$	$His^+ Uro^-$	$His^- Uro^+$	$His^- Uro^-$
Oxford	127 (77%)	8 (5%)	29 (18%)	0
Auckland	23 (33%)	17 (30%)	0	26 (37%)
Total	150 (65%)	25 (10.9%)	29 (12.5%)	26 (11.3%)

Figure 7. An unrooted phylogenetic tree showing the association of urocanate utilization with genotypes.

The capability of bacterial growth on histidine (His) and urocanate (Uro) are marked in four different colours. Number of isolates showing the same phenotype is provided in a table below the tree, and percentage of each phenotype in the Auckland, Oxford and total population is shown in parenthesis.